

Influence of geometrical and operational parameters on the axial dispersion in an aerated channel reactor

Olivier Potier*, Jean-Pierre Leclerc, Marie-Noëlle Pons

Laboratoire des Sciences du Génie Chimique, CNRS-ENSIC-INPL, 1, rue Grandville BP 20451, 54001 Nancy, France

Received 9 February 2005; received in revised form 11 August 2005; accepted 18 August 2005

Abstract

Residence time distribution experiments have been performed on an activated sludge 3000 m³ channel reactor aerated by gas diffusion (for different liquid flowrates under constant aeration rate and constant water depth) and on a bench-scale channel reactor aerated from the bottom (for different liquid and gas flowrates and water depths) in order to characterize their hydrodynamics. Both units can be modeled as plug flow reactors with axial dispersion. A general correlation has been obtained to predict the axial dispersion coefficient as a function of the gas and liquid velocities and the geometrical parameters of the full-scale and bench-scale reactors. Finally, to facilitate the simulation of biological reactions in transient state, an equivalent model based on tanks-in-series with variable back-mixing flowrate is proposed.

© 2005 Elsevier Ltd. All rights reserved.

Keywords: Aerated channel reactor; Residence time distribution; Axial dispersion coefficient; Tanks-in-series model

1. Introduction

Activated sludge process is the most widespread technique for biological wastewater treatment. In large wastewater treatment plants the aerobic degradation is often taking place in channels or closed-loop reactors (Degrémont, 1991). The channel reactor with bottom aerators is the oldest type of systems and is particularly adapted to large plants (Fig. 1a). In closed-loop processes, the mixed liquor is circulating as in a “racetrack”. They are called “oxidation ditches” when the aerators are horizontal (Fig. 1b) and “carrousel” when they are vertical (Fig. 1c). From these basic designs many variations have been proposed by various

manufacturers, by inclusion of anaerobic and anoxic zones equipped with mechanical mixing devices or as the Orbal system with several concentric ovaloid channels (Fig. 1d). Due to the shape and size of these units, there is definitely an effect of hydrodynamics on the efficiency of the pollution abatement, as concentration gradients are experimentally observed, for nutrients as well as for oxygen (Dudley, 1995). This situation can be extended to the case of facultative aerated lagoons (Dorego and Leduc, 1996). Classically channels and closed-loop reactors will have a depth of up to a few meters. An exception is the underground Henriksdal plant in Stockholm whose channels are 200 m long, 10 m wide and 12 m deep and where vertical gradients could be superposed to longitudinal effects. The effect of the flow behavior on the efficiency of wastewater treatment has been often pointed out (Metcalf and Eddy, 2002). Unfortunately, there is a limited number of correlations to predict the flow behavior. The design of such reactors

*Corresponding author. Tel.: +33 3 83 17 50 91;
fax: +33 3 83 32 73 08.

E-mail addresses: Olivier.Potier@ensic.inpl-nancy.fr
(O. Potier), marie-noelle.pons@ensic.inpl-nancy.fr (M.-N. Pons).

Nomenclature		Q_L	liquid flowrate ($L^3 T^{-1}$)
a	correlation coefficient	RTD	residence time distribution
ADM	axial dispersion model	s	Laplace variable
B	coefficient given by Eq. (17)	t	time (T)
c	tracer concentration (ML^{-3})	u	average velocity of the liquid phase inside the reactor (LT^{-1}),
CFD	computational fluid dynamics	TSM	tanks-in-series model
COD	chemical oxygen demand ($MO_2 L^{-3}$)	V	liquid phase volume
C.V.	coefficient of variation (%)	W	width (L)
d	dispersion number	x	correlation exponent
D	diffusivity ($L^2 T^{-1}$)	Y^-	coefficient given by Eq. (19)
E	dimensionless residence time distribution	Y^+	coefficient given by Eq. (20)
G	transfer function	<i>Greek letters</i>	
H	water depth (L)	α	back-mixing coefficient
J	number of mixing cells (TSM)	γ	coefficient given by Eq. (18)
J_{app}	apparent number of mixing cells	μ_i	moment of order i
$J_{appmini}$	minimal apparent number of mixing cells	μ'_i	centered moment of order i
J_{max}	maximal number of mixing cells	τ	mean residence time (T)
L	reactor length (L)	θ	dimensionless time
Pe	Peclet number		
Q_G	gas flowrate ($L^3 T^{-1}$)		

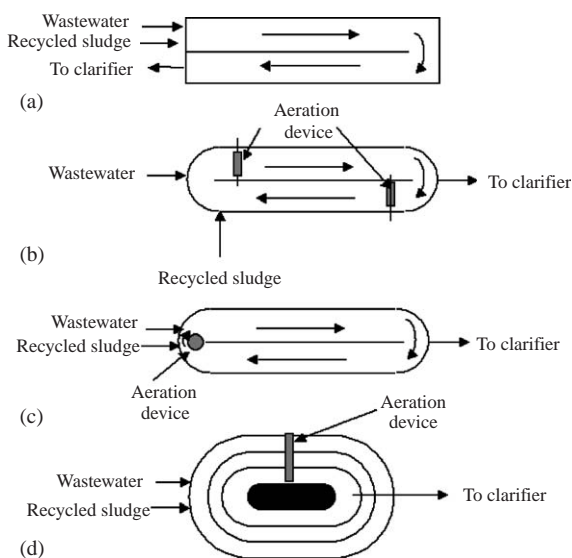


Fig. 1. Schematic representation of the different types of elongated bioreactors used in wastewater treatment plants: channel (a), oxidation ditch (b), carousel (c) and concentric channels (d).

is often based on land availability at a fixed mean residence time. Hourly data obtained on a full-scale plant (industrial data, unpublished) for the treatment of the same wastewater with the same activated sludge between 10 a.m. and 5 p.m. on a dry weather day, in two full-scale aerated channel reactors having identical mean residence times (1.75 h, C.V. = 5%) but different flow

behaviors (Peclet numbers of 16 (C.V. 6%) and 1.7 (C.V. 6%)), show that the soluble COD removal between their inlet and their outlet differs in average by 35% (C.V. 43%).

Efforts are being made to model multiphase bioreactors using Computational fluid dynamics (CFD) (Dhanasekharan et al., 2005). However, it is not yet possible to couple this approach with a complex kinetic biomodel (Henze, 2000) and simulate the behavior of full-scale plants over a long period of time. Znad et al. (2004) notice that little work has been performed on the mathematical modeling of airlift bioreactors or bubble columns. These reactors have many similarities with aerated wastewater channels, although the gas and liquid flow directions are parallel in the first case and transverse in the second case.

In channel reactors the wastewater flow behavior can be represented by two equivalent models:

- the classical plug flow reactor with axial dispersion (axial dispersion model or ADM) which contains two parameters, the mean residence time (τ) and the Peclet number (Pe) (Levenspiel, 1998)
- $Pe = \frac{uL}{D}$. (1)

The Peclet number represents the ratio of the convective flow to the diffusive one. The dispersion number

$$d = D/uL = 1/Pe, \quad (2)$$

has been considered to quantify the degree of mixing in lagoons where the treatment efficiency is modeled

through the Wehner–Wilhelm equation (Dorego and Leduc, 1996). The ADM approach produces a continuous model.

- the tanks-in-series model (TSM) which contains also two parameters; the mean residence time (τ) and the number of mixing cells (J). This discrete approach has been used by De Clercq et al. (1999) to describe the hydrodynamics in various wastewater treatment units.

In most cases the following equivalence between both models (Villiermaux, 1982) may be applied

$$Pe = 2j + 1. \quad (3)$$

Wastewater bioreactors design criteria include the food/biomass ratio (kg BOD/kg biomass day⁻¹), the BOD loading (kg BOD m⁻³ day⁻¹), the sludge age (in days) and some hydraulic data such as peak flow. The design of a reactor only based on the liquid and sludge residence times may result in large errors on the predicted efficiency of a full-scale wastewater treatment plant. Some other important features are also sensitive to hydrodynamics. For example, filamentous bulking should be limited to prevent the decrease of the settling rate in the clarifier. A plug flow behavior will favor zooglycal microorganisms and be detrimental to the overgrowth of filamentous bacteria (Chudoba et al., 1973).

The purpose of this paper is to evaluate the possibility to define a general framework to model the hydrodynamics of aerated channel reactors, taking into account the operating parameters (gas and liquid flowrate) and the geometrical parameters (length, width and mixed liquor height). For this purpose, tracing experiments have been performed in a full-scale reactor and in a bench-scale reactor. In full-scale plants, the wastewater flow-rate changes continuously with time. A day to night flowrate ratio equal to 3 can be observed (Le Bonté, 2003). The sewage system and the rainwater network are still often connected, and depending on the climate, the flowrate may vary in a proportion (with respect to summer dry weather conditions) in the range of 1–7 during heavy rain periods. Plant managers are often reluctant to change the operating conditions for specific tracer tests during normal operations as they want to avoid any accidental discharge of pollutants in receiving waters. Consequently, it is often very difficult to carry out tracing experiments in steady-state conditions. Complex flow connections between units (De Clercq et al., 1999) can make the data interpretation delicate. In order to study the effect of a large range of operating conditions and geometrical parameters, it is necessary to build a bench-scale plant. The scale-down and scale-up of multiphase bioreactors are very complex tasks. As many of them are used for shear sensitive species such as

mammalian or insect cells, shear rate is often the selected criterion (Merchuk et al., 1994; Maranga et al., 2004). Although shear has an effect on sludge flocs (Liu et al., 2005), it is certainly not as drastic as for mammalian cells and is not an issue in classical activated sludge systems. The efficiency of the aerated sludge channel reactor depends on

- the biological kinetics which depend only on the treated waste,
- the oxygen mass transfer coefficient, which depends on gas flowrate, gas hold-up, bubble size, distribution, bubble coalescence especially in deep reactors,
- the liquid residence time distribution.

Since the first two are fixed either by the biochemistry or by the production of air bubbles, the liquid residence time distribution seems to be an adequate criterion for scale-down. Obviously this choice is still debatable since it does not give any answer to the question about the conservation of the ratio of the bubble size to the characteristic dimension of the reactor.

The results obtained on a full- and a bench-scale reactor where similar liquid residence time distributions can be achieved are discussed, based on the plug flow model with axial dispersion. A semi-empirical correlation for the coefficient of dispersion has been determined to facilitate the scale-up of large reactors. To help incorporate the complex kinetics related to the bioreactions taking place in the mixed liquor, the fluctuations of the axial dispersion have been taken into account using a tanks-in-series model with back-mixing model with a constant number of cells and a variable backflow rate.

2. Materials and methods

Full-scale tests have been conducted on a 3300 m³, 100 m long, 8 m wide channel reactor, at the Nancy-Maxéville (France) plant (Fig. 2). An air diffusion system (DP230 porous discs) is fixed on its floor and provides a gas flowrate of 3350 ± 850 Nm³ h⁻¹. Three sets of experimental conditions have been selected

Run 1: heavy rain season, with a large and constant flowrate (2200 m³ h⁻¹),

Run 2: early morning, in summer time, with a small and constant flowrate (1280 m³ h⁻¹),

Run 3: late morning, with a medium and constant flowrate (1650 m³ h⁻¹).

Lithium chloride was used as an inert tracer and injected as a pulse near the entrance of the channel. Samples were grabbed on the reactor centerline from the bridges (points A, B, C, D, E, F and G) at increasing time intervals. Furthermore, samples were grabbed along the width of the reactors at the levels of points B, D and E to check for gradient. They were

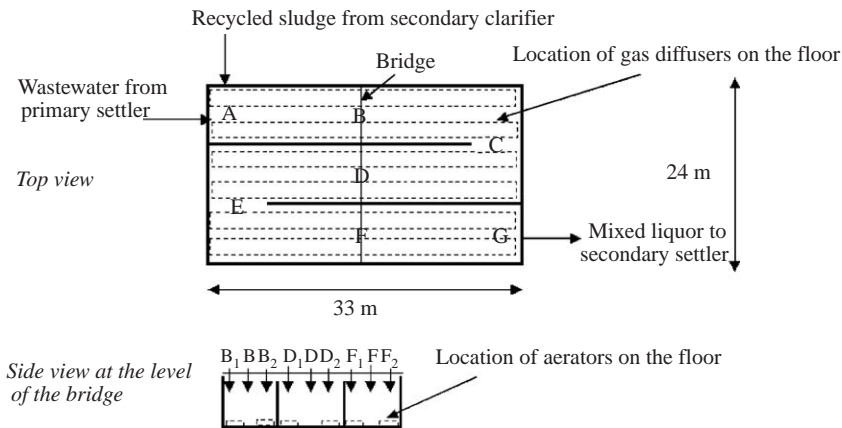


Fig. 2. Schematic representation of the full-scale aerated channel. Top and side views.

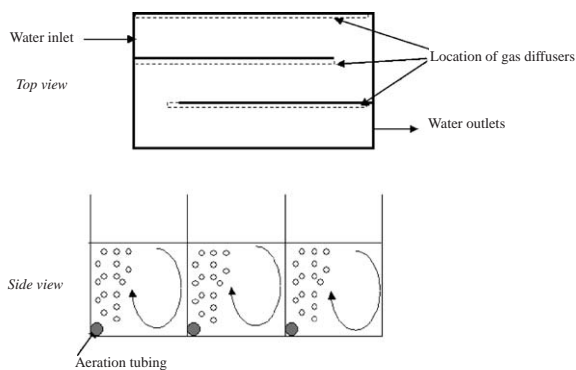


Fig. 3. Schematic representation of the bench-scale tank. Top and side views.

immediately filtrated on a $10\ \mu\text{m}$ paper filter and stored at $4\ ^\circ\text{C}$ until further analysis in 300-mL-bottles containing 1 mL of 1 M HNO_3 . Lithium content was measured by atomic absorption on a Varian AAA device, with a linear response in the range $0\text{--}6\ \text{mg L}^{-1}$ ($\pm 0.01\ \text{mg L}^{-1}$). It was verified that the tracer was not absorbed on solid matter and was non-toxic at the quantities used (10 kg of LiCl per experiment). Absorption batch tests were conducted over 24 h periods at the LiCl concentration used in the experiments and the lithium concentration variation was below $0.01\ \text{mg L}^{-1}$.

The bench-scale channel, of width $W = 0.18\ \text{m}$ and rectangular section are built in transparent materials (Plexiglas) (Fig. 3). Its total unfolded length is 3.60 m. The walls of the reactor are fitted with stainless-steel tubes where 1 mm holes have been drilled for air injection. The bubble size is of the same order of magnitude (at the injection level) in the full-scale and bench-scale channels. Due to the asymmetry, the bench-scale channel represents one half of the full-scale channel. The gas and liquid flowrates and the water

height are the variable parameters. The air flowrate (Q_G) is measured with a flow meter and can be varied between 15 and $66\ \text{L min}^{-1}$. The water depth can be adjusted by the selection of the liquid outlet position (Fig. 3). The maximal total working volume used in this study was $0.08\ \text{m}^3$. In this tank the tracing experiments have been carried out by injecting pulses of a solution of sodium chloride, the concentration of which is monitored with a conductimetric probe (Tacussel, Villeurbanne, France). The concentration of the NaCl solution was chosen so that the maximal detected concentration during the experiment was below $0.3\ \text{g L}^{-1}$.

All tracing experiments are analyzed using the software DTSPRO 4.2 (Symantec, Visp, Switzerland). The experimental Peclet number and axial diffusion coefficient are determined by curve fitting between the experimental response to the injection of the tracer and the theoretical response of the model to a pulse.

3. Results

3.1. Experimental results

The first full-scale experiment was carried out for a total liquid flowrate Q_L of $2200\ \text{m}^3\ \text{h}^{-1}$ ($0.61\ \text{m}^3\ \text{s}^{-1}$) (incoming wastewater + sludge recycle) and the results are shown in Fig. 4a. The sludge recycled from the secondary clarifiers was also monitored and its lithium concentration remained below $0.1\ \text{mg L}^{-1}$ during the whole test. Under these conditions the reactor can be represented as a plug flow reactor with axial dispersion with $Pe = 21$ (or $J = 10$ for TSM) (Fig. 4b). No gradient is observed across the width of the channel: the variation in concentrations between points B, B₁ and B₂ (respectively, D, D₁ and D₂, and E, E₁ and E₂) was below 5%. It has been verified that one-third (respectively, two-thirds) of the reactor can be modeled with

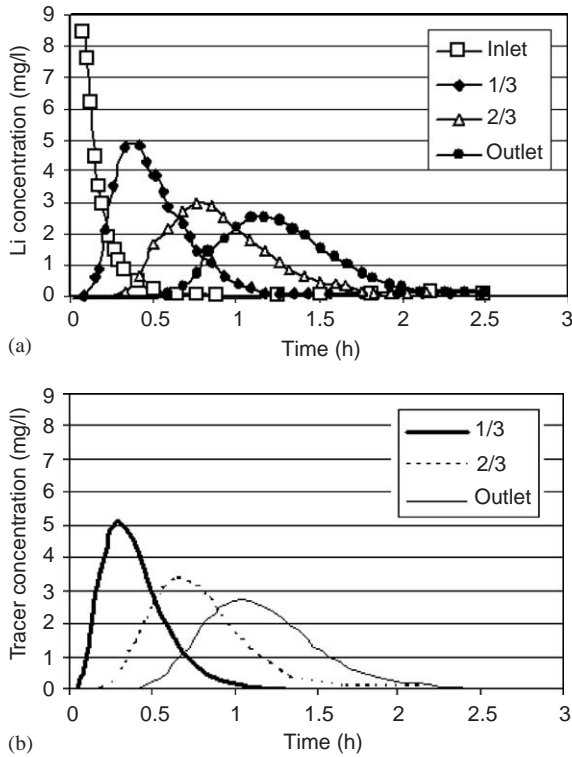


Fig. 4. Full-scale experimental RTD results (a) and corresponding simulated RTDs (b).

$Pe = 7$ (or $J = 3$), respectively, 14 (or $J = 6.5 \approx 6$). These values are much higher than those experimentally obtained by Dorego and Leduc (1996) in aerated lagoons (Pe between 2 and 3.5 for τ between 20 and 50 h). Inversely, the number of well-mixed cells found by De Clercq et al. (1999) in their tracing experiments on an industrial-activated sludge plant which has the same shape and volume as the reactor described in the present work, but with a very large τ (about 2 days) is much lower (2 but one of the cells represents more than 65% of the total tank volume).

It should be added that the differences between the lithium mass recalculated from the RTD curves at the various sampling points was below 1%, which confirms the non-absorption of lithium by the sludge at least during the experiment.

Two other experiments were subsequently carried out at $Q_L = 1650 \text{ m}^3 \text{ h}^{-1}$ ($0.46 \text{ m}^3 \text{ s}^{-1}$) and $Q_L = 1280 \text{ m}^3 \text{ h}^{-1}$ ($0.36 \text{ m}^3 \text{ s}^{-1}$), under similar aeration conditions. The corresponding values of Peclet number and the number of mixing cells J show the effect of the flowrate on the hydrodynamical regime (Fig. 6). This result is in agreement with the observation of Roustan and Line (1996), who noticed that an increase of the liquid flow induces an easier breakage of the swirls due to aeration in a channel-type reactor.

Fig. 5 presents some of the RTD curves obtained in the bench-scale tank for different liquid flowrates at a constant gas flowrate of 50 L min^{-1} with

$$E(t) = \frac{c(t)}{Q_L \int c(t) dt}, \quad (4)$$

$$\theta = t/\tau, \quad (5)$$

$$\tau = V/Q_L. \quad (6)$$

Although an exact bubble size matching between the full- and the bench-scale tanks could not be achieved, RTDs show that the channel reactor hydrodynamics are well represented by a plug flow reactor with axial dispersion model and by the perfect mixing cells in series model. The number of mixing cells J have been plotted versus the mean liquid residence time (Fig. 6). The influence of the liquid flowrate was studied by determining the Peclet number for different values of τ . A linear relation between Pe and $1/\tau$ is obtained (Fig. 7). For a given channel (width W , length L and water depth H constant) and constant gas flowrate it means that the axial dispersion coefficient remains constant as the slope is equal to L^2/D according to Eq. (10),

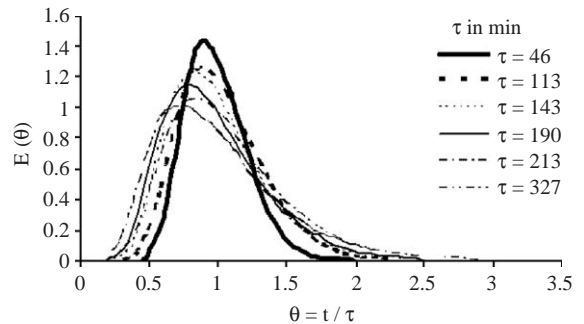


Fig. 5. Experimental RTD curves obtained on the bench-scale tank for different liquid flowrates, at constant gas flowrate.

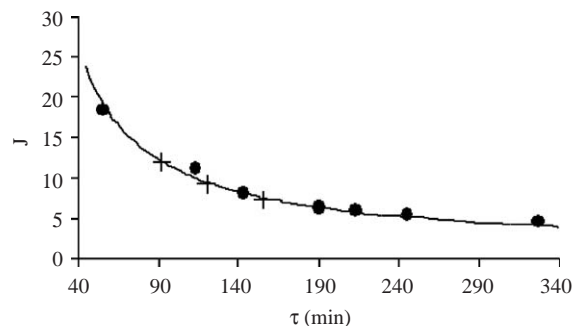


Fig. 6. Number of mixing cells, J versus liquid residence time for full-scale plant (+) and bench-scale plant (●).

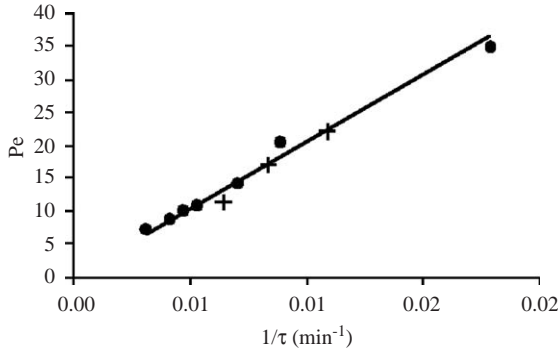


Fig. 7. Linear relationship between Pe and $1/\tau$. Full-scale plant (+) and bench-scale plant (●).

with

$$u = \frac{Q_L}{WH}, \quad (7)$$

$$\tau = \frac{V}{Q_L} = \frac{WHL}{Q_L}, \quad (8)$$

$$Pe = \frac{uL}{D} = \frac{Q_L L}{WHD}, \quad (9)$$

$$\frac{Pe}{1/\tau} = Pe\tau = \frac{Q_L L}{WHD} \frac{WHL}{Q_L} = \frac{L^2}{D}. \quad (10)$$

The influence of the air flowrate Q_G upon the axial dispersion coefficient has been studied by different authors like **Murphy and Boyko (1970)** in a channel reactor. For a given geometry of reactor, all these authors generally agree to propose the following relation where exponent x and coefficient a depend on the studied reactor:

$$D = aQ_G^x \quad \text{with } 0.3 \leq x \leq 0.5. \quad (11)$$

3.2. Correlations between the axial dispersion coefficient and the geometrical and operational parameters

In this type of experiment, the flow behavior is mainly due to the gas. The gas flowrate in the biological reactor of an activated sludge wastewater plant is very large in order to provide sufficient quantities of oxygen to bacteria and to maintain the sludge flocs in suspension. Under these conditions the momentum induced by the gas is much more important than the one induced by the wastewater flow. **Fig. 8** shows the axial dispersion coefficient versus the gas flowrate for various geometrical parameters in the bench-scale tank. The axial dispersion coefficient increases with the air flowrate but

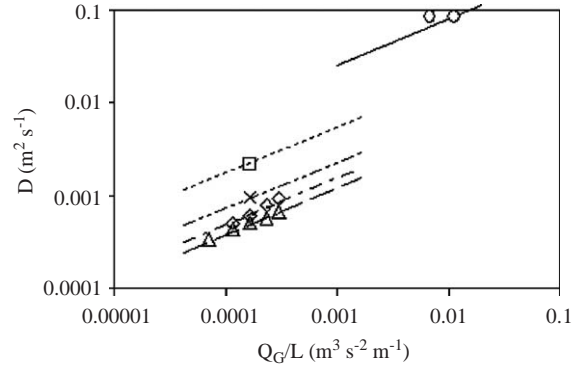


Fig. 8. Theoretical and experimental axial dispersion coefficient as a function of air flowrate per meter of channel reactor. (Δ) $H = 0.08$ m, $W = 0.18$ cm; (\diamond) $H = 0.13$ m, $W = 0.08$ m; (\times) $H = 0.08$ m, $W = 0.05$ m, (\square) $H = 0.13$ m, $W = 0.05$ m, (\circ) $H = 4$ m, $W = 4$ m.

it also depends upon geometry, especially the depth H and the width W .

Based on the experimental data, an empirical relation has been determined (Eq. (12)) for a large range of both operating and geometrical parameters.

$$D = (0.2032W - 0.008569) \left(\frac{Q_G}{L} \right)^{0.5} (100H)^{4.7310^{-3} W^{-1.99}}, \quad (12)$$

with D in $m^2 s^{-1}$, Q_G in $m^3 s^{-1}$, L , H and W in m.

The relation may often be simplified when W is large enough (Eq. (13))

$$D = (0.2032W) \left(\frac{Q_G}{L} \right)^{0.5} (100H)^{4.7310^{-3} W^{-1.99}}. \quad (13)$$

At full-scale, with large values of H and W , the correlation may be further simplified (Eq. (14))

$$D = 0.2032W \left(\frac{Q_G}{L} \right)^{0.5}. \quad (14)$$

A comparison is made with the correlation (Eq. (15)) proposed by **Murphy and Boyko (1970)** for different values of flowrate and geometrical parameters (**Fig. 9**)

$$\frac{D}{W^2} = 3.118Q_G^{0.346}, \quad (15)$$

with D in $ft^2 h^{-1}$ and Q_G in $ft^3 min^{-1}$ for $1000 ft^3$ of reacting volume (with Q_g varying between 0.002 and $200 m^3 min^{-1}$ for $1 m^3$ of reacting volume, for water depth between 0.32 and 4.5 m and channel width between 0.45 and 9 m). The comparison is difficult since the results obtained by **Murphy and Boyko** were presented 30 years ago. The gas diffusers used nowadays produce smaller gas bubbles, which induce a lower turbulence and a smaller Peclet number (i.e. a higher

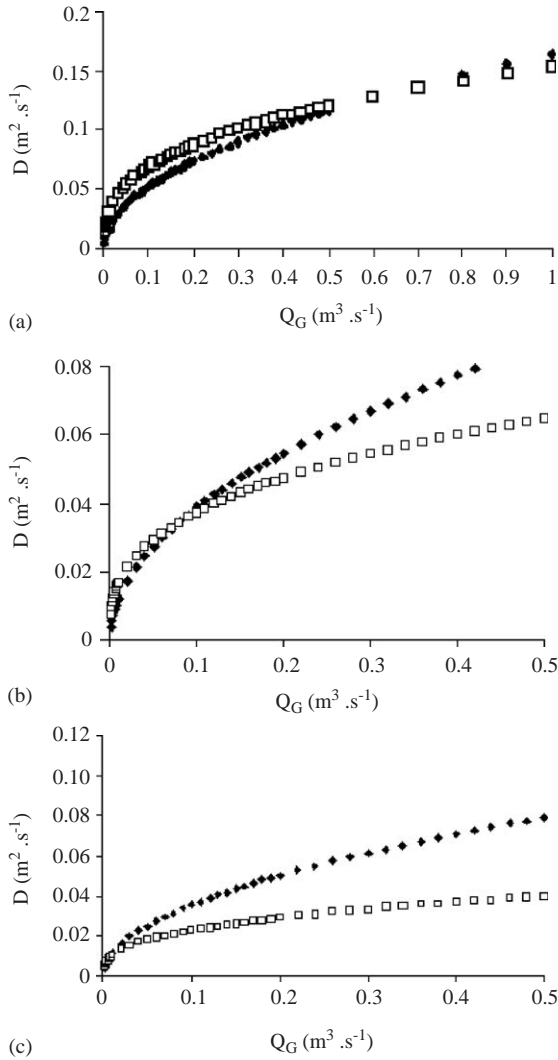


Fig. 9. Comparison between the correlation proposed in this work and the correlation proposed by Murphy and Boyko (1970) for (a) $L = 100$ m, $W = 4$ m, $H = 4$ m, (b) $L = 100$ m, $W = 6$ m, $H = 6$ m and (c) $L = 30$ m, $W = 3$ m, $H = 3$ m.

axial dispersion coefficient). Therefore the agreement is considered to be satisfactory.

3.3. Modeling with biological reactions

In order to simulate the dynamic behavior of the full-scale treatment plant, all the time variations of the wastewater characteristics (concentration and composition of polluted influent, flowrate, etc.) need to be taken into account. In the absence of any buffer tank upstream of the plant, the flowrate changes constantly. This means that the variations of the Peclet number or of the

number of cells J should be considered in the mass balances related to the biological reactions. Tanks-in-series models are usually easier to handle in simulations than distributed parameter models (Turner and Mills, 1990), although the feasibility of the ADM approach has been demonstrated for wastewater treatment plants (Makinia and Wells, 2000a, b). As mentioned previously, there is an equivalence between these two types of models. However, the calculation with a time-variable number of perfectly mixed cells leads to programming problems. Therefore an adaptation of this model based on perfect mixing cells in series with back-mixing is proposed (Fig. 10). The maximal number of mixed cells J_{max} is fixed and the change of the apparent number of mixing cells J_{app} with the flowrate is taken care of through the back-mixing coefficient α . Znad et al. (2004) have used a similar approach to model the hydrodynamics in the riser of a bio-airlift. When α is equal to 0, J_{app} is maximal and equal to J_{max} , which should be equal to the maximum value determined from the tracer experiments on a given channel reactor.

In the Laplace domain, the transfer function of the perfect mixing cells in series with back-mixing is given by

$$G(s) = (1 + \alpha) \left[\frac{1 + \alpha}{\alpha} \right]^{J_{max}-1} \left\{ \frac{2\sqrt{\gamma^2 - 4\alpha(1 + \alpha)}}{2\alpha B} \right\} \quad (16)$$

with

$$B = \left(\frac{1 + \alpha}{\alpha} \right) \left\{ \left(\frac{\gamma - \sqrt{\gamma^2 - 4\alpha(1 + \alpha)}}{2\alpha} \right)^{J_{max}-2} Y_- - \left(\frac{\gamma + \sqrt{\gamma^2 - 4\alpha(1 + \alpha)}}{2\alpha} \right)^{J_{max}-2} Y_+ \right\} \quad (17)$$

and

$$\gamma = 1 + 2\alpha + \frac{\tau \cdot s}{J_{max}}, \quad (18)$$

$$Y_- = \left[1 + \alpha + \frac{\tau \cdot s}{J_{max}} - \alpha \frac{\gamma + \sqrt{\gamma^2 - 4\alpha(1 + \alpha)}}{2\alpha} \right] \left[(1 + \alpha) - \left(1 + \alpha + \frac{\tau \cdot s}{J_{max}} \right) \frac{\gamma - \sqrt{\gamma^2 - 4\alpha(1 + \alpha)}}{2\alpha} \right], \quad (19)$$

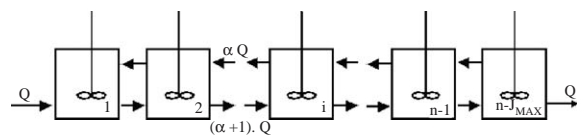


Fig. 10. Schematic representation of the tanks-in-series with back-mixing model.

$$Y_+ = \left[1 + \alpha + \frac{\tau s}{J_{\max}} - \alpha \frac{\gamma - \sqrt{\gamma^2 - 4\alpha(1 + \alpha)}}{2\alpha} \right] \left[(1 + \alpha) - \left(1 + \alpha + \frac{\tau s}{J_{\max}} \right) \frac{\gamma + \sqrt{\gamma^2 - 4\alpha(1 + \alpha)}}{2\alpha} \right]. \quad (20)$$

The moment of any transfer function may be estimated by the Van der Laan relation (Villermux, 1982)

$$\mu_n = (-1)^n \lim_{s \rightarrow 0} \frac{\partial^n G(s)}{\partial s^n}. \quad (21)$$

The second moment of the studied transfer function is written as

$$\mu_2 = \frac{\tau^2}{J_{\max}} (1 + J_{\max} + 2\alpha) - 2\alpha(1 + \alpha) \left(\frac{\tau}{J_{\max}} \right)^2 + 2 \left(\frac{\tau}{J_{\max}} \right)^2 \alpha^{1+J_{\max}} (1 - \alpha)^{1-J_{\max}}. \quad (22)$$

Since

$$\mu_1 = \bar{t}_S = \tau = \frac{V}{Q_L}, \quad (23)$$

the apparent number of mixing cells is given by

$$J_{\text{app}} = \frac{\mu_1^2}{\mu_2} = \frac{\mu_1^2}{\mu_2 - \mu_1^2}, \quad (24)$$

$$J_{\text{app}} = \frac{J_{\max}}{(1 + 2\alpha) - \frac{2\alpha(1+\alpha)}{J_{\max}} + \frac{2\alpha^{1+J_{\max}}(1+\alpha)^{1-J_{\max}}}{J_{\max}}}. \quad (25)$$

J_{app} depends only on the back-mixing flowrate for a given J_{\max} . In order to calculate α , it is necessary to make the assumption that the third term of the denominator is negligible, which will be validated below. The equation

$$2J_{\text{app}}\alpha^2 + 2J_{\text{app}}(1 - J_{\max})\alpha + J_{\max}(J_{\max} - J_{\text{app}}) = 0, \quad (26)$$

has two solutions but only one is physically acceptable (α decreases as J_{app} decreases),

$$\alpha = \frac{1}{2} \left[(J_{\max} - 1) - \left(1 + J_{\max}^2 \left(1 - \frac{2}{J_{\text{app}}} \right) \right)^{1/2} \right]. \quad (27)$$

Fig. 11 shows the relation between J_{app} and α for a given J_{\max} of 14. For a given maximal number of perfectly mixed cells, the apparent number (i.e. the Peclet number) decreases with the back-mixing rate. To validate the assumption that the third term of the denominator of Eq. 25 is negligible (i.e. $2\alpha^{1+J_{\max}}(1 + \alpha)^{1-J_{\max}}/J_{\max}$), it has been compared to $(1 + 2\alpha) - 2\alpha(1 + \alpha)/J_{\max}$, the sum of the first two terms: for J_{\max} less or equal to 18, this sum is always larger than 1, when the third term is lower than 0.014. Let us now assume

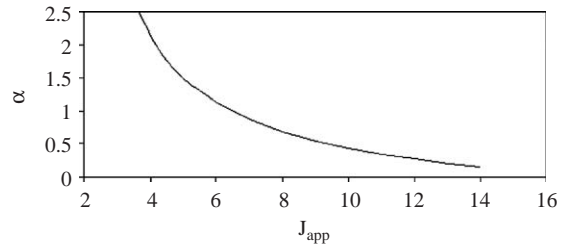


Fig. 11. Relation between J_{app} and α for $J_{\max} = 14$.

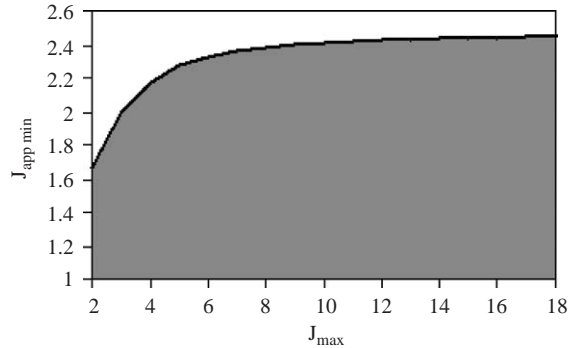


Fig. 12. Minimal value of J_{app} in function of J_{\max} .

that this third term can be neglected if it represents less than 1% of the sum of two other terms. The plot of the variation of the lower value ($J_{\text{app}} \text{ mini}$) that can be taken by J_{app} versus J_{\max} is shown in Fig. 12. For example, with J_{\max} higher than 6, J_{app} should be higher than 2.4 to use the simplified relation, which is the case in most problems.

4. Conclusion

Residence time distributions have been measured in aerated channel reactors (full-scale and bench-scale) for a large range of gas and water flowrates and geometrical parameters. For all the operating and geometrical conditions, the RTD can be represented by the tanks-in-series model or by the plug flow reactor with axial dispersion. This last model has been selected to fit the different RTD curves and to obtain the value of the dispersion coefficient for each experiment. Using the results, a general correlation has been determined to estimate the dispersion coefficient as a function of the geometrical parameters and operating parameters. For the full-scale reactor, for which the height and the width are large enough (several meters), a simplified correlation may be used.

In order to combine the biological reactions to the hydrodynamical model, an equivalence between the plug flow reactor with axial dispersion model and the perfect

mixing cells in series with back-mixing model has been demonstrated. It is possible to simulate easily the variations of the axial dispersion coefficient with the flowrate through this model with a maximal fixed number of mixing cells and a variable backflow rate.

On-going work is devoted to more complex hydrodynamics such as the case of oxidation ditches with localized aeration and anoxic channel reactors.

Acknowledgements

The authors would like to thank the staff of the LSGC workshop for the construction of the bench-scale unit and the Great Nancy Council and the plant staff for the access to the waste water treatment plant. They are also indebted to Elise Renou, Virginie Loiseau, Hélène Lallemand and Laurent Galdemas for their help in the experimental work.

References

- Chudoba, J., Ottová, V., Maděř, V., 1973. Control of activated sludge filamentous bulking—I. Effect of the hydraulic regime or degree of mixing in an aeration regime. *Water Res.* 7, 1163–1182.
- De Clercq, B., Coen, F., Vanderhaegen, B., Vanrolleghem, P.A., 1999. Calibrating simple models for mixing and flow propagation in waste water treatment plants. *Water Sci. Technol.* 39 (4), 61–69.
- Degrémont, 1991. *Water Treatment Handbook*, sixth Ed. Lavoisier, Paris.
- Dhanasekharan, K.M., Sanyal, J., Jain, A., Haidari, A., 2005. A generalized approach to model oxygen transfer in bioreactors using population balances and computational fluid dynamics. *Chem. Eng. Sci.* 60, 213–218.
- Dorego, N.C., Leduc, R., 1996. Characterization of hydraulic flow patterns in facultative aerated lagoons. *Water Sci. Technol.* 34 (11), 99–106.
- Dudley, J., 1995. Process testing of aerators in oxidation ditches. *Water Res.* 29 (9), 2217–2219.
- Henze, M., 2000. *Activated sludge models: ASM1, ASM2, ASM2d, ASM3*. IWA Publishing, London.
- Le Bonté, S., 2003. *Multivariable methods for the characterization of wastewater*. Ph.D. Thesis, National Polytechnical Institute of Lorraine (INPL), Nancy, France.
- Levenspiel, O., 1998. *Chemical Reaction Engineering*. Wiley, New York.
- Liu, Q.S., Liu, Y., Tay, J.H., Show, K.Y., 2005. Response of sludge flocs to shear strength. *Process Biochem.* 40 (10), 3202–3205.
- Makinia, J., Wells, S.A., 2000a. A general model of the activated sludge reactor with dispersive flow—I. Model development and parameter estimation. *Water Res.* 34, 3987–3996.
- Makinia, J., Wells, S.A., 2000b. A general model of the activated sludge reactor with dispersive flow—II. Model verification and application. *Water Res.* 34, 3997–4006.
- Maranga, L., Cunha, A., Clemente, J., Cruz, P., Carrondo, M.J.T., 2004. Scale-up of virus-like particles production: effects of sparging, agitation and bioreactor scale on cell growth, infection kinetics and productivity. *J. Biotechnol.* 107, 55–64.
- Merchuk, J., Ben-Zvi, S., Niranjani, K., 1994. Why use bubble-column bioreactors? *Trends Biotechnol.* 12, 501–511.
- Metcalf, M., Eddy, E., 2002. *Wastewater engineering: treatment disposal, reuse*, revised by Tchobanoglous G. Mc Graw-Hill Inc., New York.
- Murphy, K., Boyko, B., 1970. Longitudinal mixing in spiral flow aeration tanks. *J. Sanit. Eng. Div. Am. Soc. Civil Eng.* 96 (SA2), 211–221.
- Roustan, M., Line, A., 1996. Rôle du brassage dans les procédés biologiques d'épuration. *Tribune de l'Eau* 5–6/96, 109–115.
- Turner, J.R., Mills, P.L., 1990. Comparison of axial dispersion and mixing cell models for design and simulation of Fischer-Tropsch slurry bubble column reactors. *Chem. Eng. Sci.* 45, 2317–2324.
- Villermaux, J., 1982. *Génie de la réaction chimique conception et fonctionnement des réacteurs*. Tec&Doc. Lavoisier, Paris.
- Znad, H., Bálaš, V., Kawase, Y., 2004. Modeling and scale up of airlift bioreactor. *Comput. Chem. Eng.* 28, 2765–2777.